EFFECTS OF INDIUM SLABS ON THE STRUCTURAL AND ELECTRICAL PROPERTIES OF STACKED LAYERS OF Cu_2O

A. F. QASRAWI [a,b,*], A. OMAR [a]
aDepartment of Physics, Arab American University, Jenin, Palestine
bGroup of physics, Faculty of Engineering, Atilim University, 06836 Ankara, Turkey

In this work, the structural and electrical properties of stacked layers of Cu_2O that comprises indium slabs in its structure are reported. The stacked layers which are coated onto glass and Au substrates under vacuum pressure of 10^{-5} mbar are characterized by the X-ray diffraction and impedance spectrometry techniques. While the Cu_2O/Cu_2O (CC) layers exhibited amorphous nature of growth, those which contained indium slabs (CIC) displayed weak crystallinity. The insertion of indium slabs between stacked layers of cuprous oxide highly increased the electrical resistivity and shifted the acceptor level closer to the valance band edge. In addition, the analyses of the conductance and capacitance spectra in the frequency domain of 0.01-1.0 GHz have shown that these two physical parameters are strongly affected by the insertion of indium slabs and by surface deformation effects. The capacitance spectra showed negative capacitance effect (NC) in all the studied frequency domain. The NC effects become less pronounced in the CIC samples owing to the changes in the polarization mechanism. The feature of NC effects make both of the CC and CIC samples more appropriate for electronic and telecommunication technology as it can be used in amplifiers to enhance he gain, as parasitic cancellers and as noise reducers.

1. Introduction

Cuprous oxide thin films have been under the focus of research centers owing to their applicability in electronics and optoelectronics. They have been used as switching memories [1], as solar cells [2] and as gas sensors [3]. It was shown that heterojunction devices made of $Pt/CsPbBr_3/Cu_2O/FTO$ exhibit significant switching effect that make them suitable as an efficient electric storage materials in RRAM devices [1]. In addition, perovskite solar cells that contain Cu_2O nono-cubes on its top surface are reported to achieve an efficiency of ~17% [2]. This achievement makes the Cu_2O layers promising and worthy of consideration as well performing solar cells. Moreover, as gas sensors, while the pristine CuO/Cu_2O gas sensors show high gas sensitivity. Insertion of Ag metal to form nano-channels of $CuO/Cu_2O/Ag$ enhanced the gas sensitivity by a factor of 7.3 [3]. These sensors showed sensitivity of 8.04 at 125 parts per billion for acetone analytes.

Literature data reported information about the ability of doping agents to engineer the physical properties of cuprous oxide. As for examples, doping cuprous oxide with Sb makes the material effectively shares in the fabrication of quantum dot light emitting diodes [4]. In addition, N doping to Cu_2O films which are coated onto SnO_2 substrates leads to the high light transparency and forces it to exhibit excellent photovoltaic properties [5]. The features and applications of Cu_2O motivated us to attempt to investigate its electrical properties using a different way of doping. Particularly, here in this work, two tacked layers of Cu_2O which are coated onto glass and Au substrates are sandwiched with indium slabs of thicknesses of 100 nm. The $Cu_2O/In/Cu_2O$ films are structurally and electrically studied to explore the changes in the crystalline nature, the electrical resistivity, and conductance and capacitance spectra in the frequency domain of 0.01-1.0 GHz.

_____
*Corresponding author: atef.qasrawi@atilim.edu.tr

2. Experimental details

Cuprous oxide thin films are grown onto ultrasonically cleaned glass substrates with the help of a VCM-600 vacuum evaporator under vacuum pressure of 10^{-5} mbar. The evaporated materials were high purity (99.9995%) Cu_2O powders (Alfa Aeser). The coating started with a Cu_2O layer of thickness of 500 nm. The produced Cu_2O film was covered with 100 nm thick indium layers. The produced Cu_2O/In two stacked layers is used as substrate to grow a third layer of Cu_2O of thickness of 500 nm. The size of the indium slabs represents 10% of the total volume of the films. Some of the glass/Cu_2O films were coated with another Cu_2O layer without insertion of indium slabs to allow exploring the indium slabs effect. The films thicknesses (d) are monitored with the help of an in situ INFICON STM-2 thickness monitor. The films were characterized with the help of Miniflex 600 X-ray diffraction unit, homemade high temperature cryostat and Agilent 4291B 10-1800 MHz impedance analyzer.

3. Results and discussion

The effect of insertion of indium slabs on the structural properties of two stacked layers of copper oxide (CC) which are coated onto Au substrates is evident from the X-ray diffraction patterns that are shown in Fig. 1. As can be seen from the figure, sharp reflection peaks appears at different diffraction angles (2θ). The analyses of these patterns were actualized with the help of "Crystdiff" software packages using the lattice parameters which are published in literature or crystallography database cards. The orthorhombic Cu_2O [6], cubic Cu_2O (PDF card No.: 00-005-0667), monoclinic CuO (PDF card No. 74-1021), tetragonal indium (PDF card No.: 00-005-0642), body centered cubic In_2O_3 (PDF card No. 06-0416), cubic Au (PDF card No. 65-2870) and orthorhombic Au_2O_3 were tested. The tests revealed the possible reflection planes which are indexed in the figure. In accordance with the estimated reflection lists of these materials, the cubic Au reflection planes are strongly dominant indicating the crystalline nature of the substrate. The peak centered at $2\theta = 35.1^o$ are assignable to the orthorhombic Cu_2O. In addition, since both of the CuO and Au exhibit maximum diffraction patterns at $2\theta = 38.95^o$, it is not easily possible to decide whether the strong reflections at this angle is related to monoclinic CuO or cubic Au. However, as the strongest peak (100%) of monoclinic CuO appears at $2\theta = 32.53^o$ and the reflection peak of monoclinic CuO which appears at $2\theta = 38.95^o$ exhibit relative intensity of 25%, it turn out to be more appropriate to assign this peak to face centered cubic gold. It is also clear from Fig. 1, that the XRD patterns of the Cu_2O stacked layers which comprises indium in its structure (CIC), peaks of tetragonal indium appears guaranteeing the presence of polycrystalline indium in the structure of the samples.
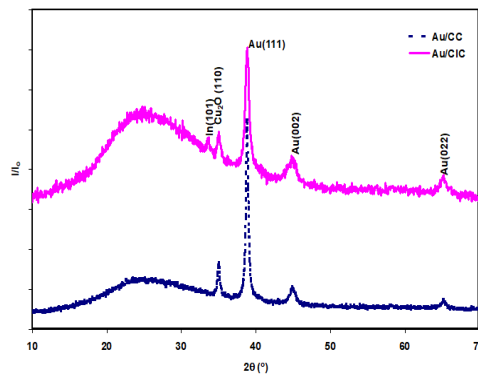

Fig. 1. the X-ray diffraction patterns for Au/Cu₂O/Cu₂O, for Au/Cu₂O/In/Cu₂O stacked layers.

Even though the XRD patterns indicated the presence of polycrystalline orthorhombic Cu_2O in the structure of the films, the nonappearance of more reflection peaks necessarily indicates the growth of polycrystalline material in an amorphous sea of Cu_2O. It is also worth mentioning that the XRD measurements on the samples which are grown onto glass substrates (not shown) did not display any sharp reflections indicating the amorphous nature of growth of the CC and CIC films. The reason beyond the crystallinity of the Cu_2O films which are coated onto Au substrates is the metal induced crystallization process which is initiated by Au. The metal induced crystallization process is believed to be driven by the reduction of the free energy of the materials during
the transformation from the amorphous to the crystalline phase [7]. It can be actualized by the layer exchange mechanisms and/or diffusion assisted crystallization. The ionic radius of Au^{+1} being 137 pm [8] is much larger than that of Cu^{+1} (60 pm [9]) indicating that diffusion of Cu atoms into Au vacant sites is possible and the reverse substitutions are not expected. The value of the bond length of Au–Cu being 233 pm is less than 253 pm (Au–Au length of Au_2) and larger than 218 pm (Cu–Cu length of Cu_2) indicating the possibility of alloying of an Au atom with a Cu atom [10]. This mechanism is reported to cause stronger interactions leading to the atomic displacement which result in better crystallization process.

Fig.2 illustrates the Arrhenius plot of the direct current electrical resistivity (ρ) – temperature (T) variations for the glass/CC and glass/CIC amorphous samples (geometry is shown in the inset of Fig. 2). The resistivity is studied in the temperature range of 300-420 K. The room temperature values of the electrical resistivity of CC and CIC samples are found to be 0.45 and 4.14×10^6 (Ωcm), respectively. It is clear from these values that the insertion of indium slabs has significantly affected the electrical resistivity values. The literature data display electrical resistivity values that depends on the growth conditions in the range of 10^{-3}-10^6 (Ωcm) [11-13] for a single layer of Cu_2O. On the other hand, the slope of the $\ln(\rho) - T^{-1}$ variations in accordance with the Arrhenius equation, $\rho(T) \propto \exp(E_\rho/kT)$ reveal resistivity activation energy of values of 0.40 and 0.25 eV for CC and CIC samples, respectively. These activation energy values which are less than half of the energy band gap (E_g=2.17 eV [13]) indicate the extrinsic nature of conduction and it is usually assigned as an acceptor/or donor level above the valence or below the conduction band, respectively. The Fermi level is assumed to be at midpoint between the relative band and the acceptor/donor center. From this point of view, for the p −type CC layers, the work function ($q\varphi = q\chi + E_g - |E_v - E_F|$) is 6.04 eV. The electron affinity ($q\chi$) for Cu_2O is reported to be 4.07 eV [14]. Since the indium metal work function being 4.23 eV is less than the work function of p-type Cu_2O, the In/Cu_2O represents a Schottky nature of contact. However, as indium is sandwiched between two layers of Cu_2O it behave as back to back Schottky diode which when forward biased it reduces the value of the direct current significantly [15]. The current reduction leads to high resistance value which in turn explains the reason beyond the abrupt increase in the electrical resistivity values upon indium sandwiching. It is still worth remembering that these samples (CC and CIC) which are coated onto glass substrates are of amorphous nature indicating that the participation of indium in the structure of Cu_2O may lead to a shift in the extended band tails which exists in the band gap of Cu_2O films. Band tails of width of 0.60 eV are reported to exist in pure Cu_2O [16]. This belief is confirmed from the shift in the resistivity activation energy from 0.40 to 0.25 eV upon insertion of indium slabs.
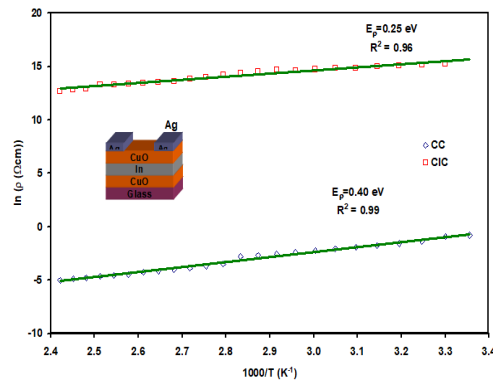
Fig. 2 the logarithmic plots of electrical resistivity for the Cu₂O/Cu₂O and Cu₂O/In/Cu₂O stacked layers which are coated onto glass substrates. The inset shows the geometrical design of the samples used through resistivity measurements.

From practical point of view, measuring the features of the ac signal propagation in the samples, opens the doors for using the CC and CIC samples as radio/microwave cavities. For this purpose, samples which are coated onto Au substrates were re-contacted in accordance with the geometrical design which is shown the inset of Fig. 3 (a). The Au/CC/Ag and Au/CIC/Ag interfaces where imposed between the electrodes of an impedance analyzer to measure the conductance (G) and capacitance (C) responses in the frequency domain of 0.01-1.0 GHz. The resulting spectra of G and C are shown in Fig. 3 (a) and (b), respectively. It is clear from Fig. 3 (a) that the conductance of the CC samples decreases upon insertion of indium slabs. The conductance of the CC samples follow two trends of variations in response to the ac signal frequency values. Namely, the logarithmic slope of the $G - f$ variation which follows the relation, $\propto f^s$, reveal s values of -1.45 and -1.65 in the frequency domain of 0.10-1.0 GHz. This style of variation was previously observed in Al/Al₂O₃/PVA:n-ZnSe (PVA: polyvinyl alcohol) Schottky barrier diodes and was owed to the presence of interface states. The interface states is mentioned depending on a number of factors such as the structure quality of material, presence of oxide layer and size of diode. Mostly, the presence of residual strain or micro- deformation is a main contribution for the dynamic behavior of conductance [17]. Similar behavior of frequency dependent AC conductance was also observed for exfoliated graphite [18]. In these samples, the conductivity slowly decreased with increasing frequency up to 0.5 MHz and then sharply decreases with increasing frequency values in the range of 0.5-3.0 MHz. The behavior is attributed to the skin effects. The skin effect arises from the decreasing excursion of charges that are responsible for the polarization as the frequency increases and the consequent reduced degree of electrical connectivity across the carbon–contact interface [18].
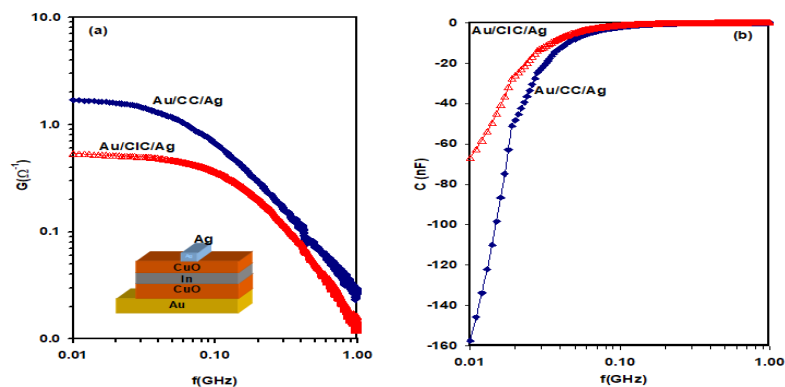

Fig. 3. The conductance and capacitance spectra for the Au/Cu₂O/Cu₂O and Au/Cu₂O/In/Cu₂O films in the frequency domain of 0.01-1.0 GHz. The inset shows the geometrical design for capacitance and conductance measurements.

On the other hand, Fig. 3 (b) displays the capacitance spectra for both of the samples before and after the insertion of indium slabs. In general, the samples exhibit negative capacitance effect (NC). The negative capacitance plays important roles in cases where signal's noise reduction [19, 20] and parasitic capacitance cancellation is required. NC effect is used for enhancing the gain distribution in amplifiers [21]. The NC effect is attributed to deformations presented by the strain and defect densities. Generally, defects lead to an increase in the trap states at the interface [20]. The NC effects decreases as the indium slabs were inserted between layers of Cu_2O. In other words, the negative capacitance becomes less negative in the CIC samples. This behavior may be owed to the changes in the polarization mechanism in the presence of indium atoms. It is mentioned that in energy-efficient versatile memories that get benefit from negative capacitance effect, the NC effect is remarkably affected by the polarization and depolarization of ferroelectric switching along the direction of vertical electric field [22]. It turns out to be worth remembering that the insertion of indium slabs which have tetragonal structure adds extra deformation and alters the bonding mechanism in the Cu_2O samples. These changes may have resulted in changes in the polarization/depolarization directions and degrees leading to the reduction in the negativity of the capacitance.

4. Conclusions

In this study, we reported the structural and electrical properties of the as grown samples of Cu_2O that comprises indium slabs of thicknesses of 100 nm. In general, stacking of layers of Cu_2O onto glass substrates does not alter the amorphous nature of the films and caused deep acceptor levels in the band gap of Cu_2O. The acceptor levels shifts toward the valance band upon insertion of indium slabs. Such property is accompanied with large increase in the electrical resistivity of Cu_2O. In addition, the Cu_2O stacked layers which are deposited onto polycrystalline Au substrates, displayed weak crystallinity in an amorphous sea. The features of these samples nominate the stacked layers of Cu_2O for use in thin film transistor technology as high gain amplifiers, noise reducers, memory switches and parasitic capacitance cancellers.

References

[1] B. Li, W. Hui, X. Ran, Y. Xia, F. Xia, L. Chao, Y. Chen, W. Huang, J. Mater. Chem. C 2019, https://doi.org/10.1039/C9TC02233C.

[2] A. M. Elseman, M. S. Selim, L. Luo, C. Y. Xu, G. Wang, Y. Jiang, D. B. Liu, L. P. Liao, Z. Hao, Q. Song, Chem. Sus. Chem. **12**(16), 3808 (2019).

[3] Y. M. Choi, S. Y. Cho, D. Jang, H. J. Koh, J. Choi, C. H. Kim, H. T. Jung, Adv. Funct. Mater. **29**(9), 1808319 (2019)

[4] H. J. Seo, J. E. Lee, S. B. Heo, M. Kim, Y. Yi, S. J. Kang, SH. K. Kim, Phys. Status Solidi A, 1900004 (2019).

[5] J. Pan, S. Li, Y. Liu, W. Ou, H. Li, W. Zhao, J. Wang, C. Song, Y. Zheng, C. Li, Chem. Eng. J. **382**, 122813 (2020).

[6] P. Scardi, M. Leoni, M., Mat. Sci. Eng. A **393**(1-2), 396 (2005)

[7] A. M. Mahamad, G. K. Mamidipudi, Crystallization-Science and Technology, 461 (2012).

[8] C. Thieme, M. Kracker, C. Patzig, K. Thieme, C. Rüssel, T. Höche, J. Eur. Ceram. Soc. 39(2-3), 554 (2019).

[9] R. Chetty, A. Bali, M. H. Naik, G. Rogl, P. Rogl, M. Jain, S. Suwas, R. C. Mallik, Acta Mater. **100**, 266 (2015).

[10] Z. Y. Jiang, Z.Y. Zhao, Catal. Sci. Technol. **7**(23), 5709 (2017)

[11] F. Gao, R. Gao, H. Liu, Z. Yang, X. Hua, X. Wu, arXiv preprint arXiv **1905**, 03432 (2019).

[12] K. Kamli, Z. Hadef, B. Chouial, B. Hadjoudja, B Surf. Eng. **35**(1), 86 (2019).

[13] O. Madelung, Semiconductors: data handbook. Springer Science & Business Media, 2012.

[14] S. S. Jeong, A. Mittiga, E. Salza, A. M. Masci, S. Passerini, SElectrochim. Acta, **53**(5), 2226 (2008).

[15] S. M. Sze, K. K. Ng, Physics of semiconductor devices. John wiley & sons, 2006.

[16] I. Y. Bouderbala, A. Herbadji, L. Mentar, A. Beniaiche, A. Azizi, J. Electron. Mater. **47**(3), 2000 (2018).

[17] M. Sharma, S. K. Tripathi, Mat. Sci. Semicon. Proc. **41**, 155 (2016).

[18] X. Hong, D. D. L. Chung, Carbon **91**, 1 (2015).

[19] N. Zagni, P. M. Pavan, M. A. Alam, M Appl. Phys. Lett. **114**(23), 233102 (2019)

[20] A. F. Qasrawi, H. D. Aloushi, Mater. Res. Express **6**(8), 086435 (2019)

[21] A. Ghadiri, K. Moez, K., IEEE T. Circuits. I **57**(11), 2834 (2010).

[22] Y. C. Chiu, C. H. Cheng, G. L. Liou, C. Y. Chang, IEEE T. Electron Dev. **64**(8), 3498 (2017).